Available online at www.sciencedirect.com
SCIENCE DIRECT®
PERGAMON
Polyhedron 22 (2003) 1633–1639
POLYHEDRON
www.elsevier.com/locate/poly

Metal complexes of *meso*-tetra-(*p*-chlorophenyl)porphyrin and *meso*-tetra-(*p*-bromophenyl)porphyrin: Tl[(*p*-Cl)$_4$tpp](OAc) and In[(*p*-X)$_4$tpp](OAc) [X = Cl, Br, tpp = 5,10,15,20-tetraphenylporphyrinate]

Yu-Yi Lee [a], Jyh-Horung Chen [a], Hsi-Ying Hsieh [b,*]

[a] *Department of Chemistry, National Chung-Hsing University, Taichung 40227, Taiwan, ROC*
[b] *Chung Hwa College of Medical Technology, Tainan 717, Taiwan, ROC*

Received 7 January 2003; accepted 21 February 2003

Abstract

The crystal structures of acetato-[*meso*-tetra(*p*-chlorophenyl)porphyrinato]thallium(III) Tl[(*p*-Cl)$_4$tpp](OAc) (**1**), acetato-[*meso*-tetra(*p*-chlorophenyl)porphyrinato]indium(III) In[(*p*-Cl)$_4$tpp](OAc) (**2**) and acetato-[*meso*-tetra(*p*-bromophenyl)porphyrinato]indium(III) In[(*p*-Br)$_4$tpp](OAc) (**3**) were determined. The coordination sphere around the Tl^{3+} ion in **1** is described as six-coordinate distorted square-based pyramid in which the apical site is occupied by a chelating bidentate OAc^- group, whereas for the In^{3+} ion in **2** and **3**, it is a five-coordinate regular square-based pyramid in which the unidentate OAc^- ligand occupies the axial site. The plane of the four pyrrole nitrogen atoms [i.e. N(1)–N(4)] strongly bonded to Tl^{3+} (or In^{3+}) is adopted as a reference plane 4N. The Tl^{3+} is moderately out of the 4N plane; its displacement of 0.69 Å is in the same direction as that of the acetate oxygen for **1**. The In^{3+} are located at 0.57 Å from its 4N plane for **2** and **3**. The free energy of activation at the coalescence temperature T_c for the intermolecular acetate exchange for **1** in CD_2Cl_2 is found to be $\Delta G^{\neq}_{200} = 42.54$ kJ mol^{-1} whereas the intermolecular OAc^- exchange for acetato-[*meso*-tetra(*p*-bromophenyl)porphyrinato]thallium(III) Tl[(*p*-Br)$_4$tpp](OAc) (**4**) in CD_2Cl_2 is determined to be $\Delta G^{\neq}_{200} =$ 42.46 kJ mol^{-1} through ^{1}H NMR temperature-dependent measurements. Moreover, the two oxygen atoms of the acetato group for **2** and **3** are asymmetrically and chelating bidentately bound to the indium atom in CD_2Cl_2 (or $CDCl_3$) solvent.

Keywords: Crystal structures; Thallium *meso*-tetra-(p-chlorophenyl)porphyrin; Indium *meso*-tetra-(p-chlorophenyl)porphyrin; Indium *meso*-tetra-(p-bromophenyl)porphyrin

1. Introduction

Our earlier work reported on the molecular structures of (acetato)(*meso*-tetraphenylporphyrinato)thallium(III) Tl(tpp)(OAc) [1,2] and (acetato)(*meso*-tetraphenylporphyrinato)indium(III) In(tpp)(OAc) [3]. The electron density and the donating ability of the pyrrole nitrogen, which is the first bonding atom toward the thallium (or indium) ion in the thallium (or indium) porphyrin complex, are considered to be lowered in the case of H$_2$(*p*-Cl)$_4$tpp [or H$_2$(*p*-Br)$_4$tpp], as it contains an electron-withdrawing chlorine (or bromine) atom [4]. Upon replacing tpp^{2-} with (*p*-Cl)$_4$tpp^{2-} and (*p*-Br)$_4$-tpp^{2-}, the complex Tl(tpp)(OAc) became acetato-[*meso*-tetra(*p*-chlorophenyl)porphyrinato]thallium(III) Tl[(*p*-Cl)$_4$tpp](OAc) (**1**) and acetato-[*meso*-tetra(*p*-bromophenyl)porphyrinato]thallium(III) Tl[(*p*-Br)$_4$tpp]-(OAc) (**4**), and complex In(tpp)(OAc) became acetato-[*meso*-tetra(*p*-chlorophenyl)porphyrinato]indium(III) In[(*p*-Cl)$_4$tpp](OAc) (**2**) and acetato-[*meso*-tetra(*p*-bromophenyl)porphyrinato]indium(III) In[(*p*-Br)$_4$tpp]-(OAc) (**3**). The acetate is bidentately coordinated to the Tl and In atom in Tl(tpp)(OAc) and In(tpp)(OAc), respectively. However, the introduction of Cl (or Br) in the *para* position of the benzene ring of complexes **1**–**4** might cause a change in the bonding of the acetate to the Tl atom in **1**, **4** and to the In atom in **2**, **3** from the

* Corresponding author.

0277-5387/03/$ - see front matter
doi:10.1016/S0277-5387(03)00330-9

chelating bidentate type as observed in Tl(tpp)(OAc) and In(tpp)(OAc).

In this paper, we reported the X-ray structural determination of three new porphyrin complexes namely **1**, **2** and **3**. Prompted by the earlier studies on the acetate exchange of Tl(tpp)(OAc) observed in CD_2Cl_2, we investigated a similar intermolecular exchange for complexes **1** and **4** in CD_2Cl_2 by ^1H and ^{13}C dynamic NMR methods.

2. Experimental

2.1. Preparation of Tl[(p-Cl)$_4$tpp](OAc) (1)

A mixture of H_2[(*p*-Cl)$_4$tpp] (0.1 g, 1.33×10^{-4} mol) in CH_2Cl_2 (50 ml) and $Tl(OAc)_3$ (0.15 g, 3.99×10^{-4} mol) in MeOH (10 ml) was refluxed for 1 h. After concentrating, the residue was dissolved in CH_2Cl_2, dried over anhydrous Na_2SO_4 and filtered. The filtrate was layered with MeOH to afford purple crystals of **1** (0.13 g, 87%) for single-crystal X-ray analysis.

^1H NMR (599.95 MHz, CD_2Cl_2, 20 °C): δ 9.06 [d, H_β, ^4J(Tl–H) = 64 Hz], 8.25 [d, ^3J(H–H) = 8 Hz] and 8.04 [d, ^3J(H–H) = 8 Hz] for phenyl *ortho* protons (*o*-H); 7.79 [d, ^3J(H–H) = 8 Hz] and 7.71 [d, ^3J(H–H) = 8 Hz] for phenyl *meta* protons (*m*-H); −0.02 (s, OAc). ^1H NMR (599.95 MHz, CD_2Cl_2, −90 °C): δ 9.07 [d, H_β, ^4J(Tl–H) = 64 Hz], 8.19 [d, ^3J(H–H) = 8 Hz] and 7.97 [d, ^3J(H–H) = 8 Hz] for phenyl *ortho* protons (*o*-H); 7.74 [d, ^3J(H–H) = 8 Hz] and 7.62 [d, ^3J(H–H) = 8 Hz] for phenyl *meta* protons (*m*-H); −0.06 [d, OAc, ^4J(Tl–H) = 14.4 Hz]. ^{13}C NMR (125.70 MHz, $CDCl_3$, 20 °C): δ 173.7 (s, OAc–CO); 149.8 [d, C_α, ^2J(Tl–C) = 15 Hz]; 140.2 [d, C_1, ^4J(Tl–C) = 27 Hz]; 136.0 [d, ^5J(Tl–C) = 22 Hz] and 135.3 [d, ^5J(Tl–C) = 22 Hz] for phenyl-$C_{2,6}$; 134.6 (s, C_4); 132.5 [d, C_β, ^3J(Tl–C) = 119 Hz]; 127.0 (s, $C_{3,5}$); 120.9 [d, C_m, ^3J(Tl–C) = 146 Hz]; 18.3 (s, OAc–Me). ^{13}C NMR (150.87 MHz, CD_2Cl_2, −90 °C): δ 173.8 [d, OAc–CO, ^2J(Tl–C) = 242 Hz]; 148.7 [d, C_α, ^2J(Tl–C) = 16 Hz]; 139.1 [d, C_1, ^4J(Tl–C) = 27 Hz]; 135.5 [d, ^5J(Tl–C) = 21 Hz] and 135.2 [d, ^5J(Tl–C) = 21 Hz] for phenyl-$C_{2,6}$; 133.3 (s, C_4); 132.2 [d, C_β, ^3J(Tl–C) = 117 Hz]; 126.5 (s) and 126.4 (s) for $C_{3,5}$; 120.3 [d, C_m, ^3J(Tl–C) = 146 Hz]; 17.7 [d, OAc–Me, ^3J(Tl–C) = 292 Hz]. MS, *m*/*z* (assignment, rel. intensity): 1158 ([Tl(*p*-Cl)$_4$tpp(OAc)]$^+$, 1.56), 955 ([Tl(*p*-Cl)$_4$tpp]$^+$, 36.87), 752 ([H(*p*-Cl)$_4$tpp]$^+$, 25.21). UV–Vis spectrum, λ (nm) [$\varepsilon \times 10^{-4}$ (M^{-1} cm^{-1})] in CH_2Cl_2: 336 (23.5), 434 (205), 568 (19.2), 607 (10.2).

2.2. Preparation of In[(p-Cl)$_4$tpp](OAc) (2)

Free base H_2[(*p*-Cl)$_4$tpp] (0.1 g, 1.33×10^{-4} mol) and In_2O_3 (0.11 g, 1.45×10^{-4} mol) were refluxed for 12 h in 50 cm^3 of acetic acid. After concentrating, the residue was dissolved in CH_2Cl_2, dried over anhydrous Na_2SO_4 and filtered. The filtrate was layered with MeOH to afford purple crystals of **2** (0.116 g, 84%) for single-crystal X-ray analysis. ^1H NMR (499.85 MHz, $CDCl_3$, 20 °C): δ 9.02 (s, H_β, 8.31 [d, ^3J(H–H) = 7 Hz] and 8.02 [d, ^3J(H–H) = 7 Hz] for phenyl *ortho* protons (*o*-H); 7.78 [d, ^3J(H–H) = 8 Hz] and 7.72 [d, ^3J(H–H) = 8 Hz] for phenyl *meta* protons (*m*-H); 0.06 (s, OAc). ^{13}C NMR (125.70 MHz, $CDCl_3$, 20 °C): δ 176.0 (s, OAc–CO); 149.5 (s, C_α); 140.3 (s, C_1); 136.0 (s) and 135.2 (s) for phenyl-$C_{2,6}$; 134.5 (s, C_4); 132.5 (s, C_β); 127.0 (s, $C_{3,5}$); 120.4 (s, C_m); 18.2 (s, OAc–Me). MS, *m*/*z* (assignment, rel. intensity): 1017 ([In(*p*-Cl)$_4$tpp(OAc)]$^+$, , 5.21), 865 ([In(*p*-Cl)$_4$tpp]$^+$, 100), 753 ([H_2(*p*-Cl)$_4$tpp]$^+$, 10.22). UV–Vis spectrum, λ (nm) [$\varepsilon \times 10^{-4}$ (M^{-1} cm^{-1})] in CH_2Cl_2: 326 (4.4), 406 (8.9), 427 (135.8), 561 (4.6), 600 (1.7).

2.3. Preparation of In[(p-Br)$_4$tpp](OAc) (3)

Compound **3** in 66% yield was prepared in the same way as described for **2** using H_2[(*p*-Br)$_4$tpp]. Compound **3** was dissolved in CH_2Cl_2 and layered with MeOH to obtain purple crystals for single-crystal X-ray analysis. ^1H NMR (599.95 MHz, $CDCl_3$, 20 °C): δ 9.03 (s, H_β, 8.26 (d) and 8.24 (d) for phenyl *ortho* protons (*o*-H); 7.96–7.93 (m) for phenyl *ortho* and *meta* protons; 7.85 (d) and 7.86 (d) for phenyl *meta* protons (*m*-H); −0.08 (s, OAc). ^{13}C NMR (150.87 MHz, $CDCl_3$, 20 °C): δ 176.3 (s, OAc–CO); 149.4 (s, C_α); 140.8 (s, C_4); 136.3 (s) and 135.5 (s) for phenyl-$C_{2,6}$; 132.5 (s, C_β); 129.9 (s, $C_{3,5}$); 122.8 (s. C_1); 120.4 (s, C_m); 18.1 (s, OAc–Me). MS, *m*/*z* (assignment, rel. intensity): 1043 ([In(*p*-Br)$_4$tpp]$^+$, 21.64); 963 ([In(*p*-Br)$_4$tpp–Br]$^+$, 3.32). UV–Vis spectrum, λ (nm) [$\varepsilon \times 10^{-4}$ (M^{-1} cm^{-1})] in CH_2Cl_2: 325 (60), 407 (113), 419 (139), 523 (9.8), 562 (61), 602 (26).

2.4. Preparation of Tl[(p-Br)$_4$tpp](OAc) (4)

Compound **4** was prepared in the same way as described for **1** using H_2[(*p*-Br)$_4$tpp]. ^1H NMR (600.13 MHz, CD_2Cl_2, 20 °C): δ 9.05 [d, H_β, ^4J(Tl–H) = 63 Hz], 8.19 [d, ^3J(H–H) = 8 Hz] and 7.99 [d, ^3J(H–H) = 8 Hz] for phenyl *ortho* protons (*o*-H); 7.94 [d, ^3J(H–H) = 8 Hz] and 7.88 [d, ^3J(H–H) = 8 Hz] for phenyl *meta* protons (*m*-H); −0.04 (s, OAc). ^1H NMR (600.13 MHz, CD_2Cl_2, −90 °C): δ 9.07 [d, H_β, ^4J(Tl–H) = 64 Hz]; 8.11 [d, ^3J(H–H) = 8 Hz] for *o*-H; 7.88 (m) for *o*-H and *m*-H; 7.75 [d, ^3J(H–H) = 8 Hz] for phenyl *meta* protons (*m*-H); −0.08 [d, OAc, ^4J(Tl–H) = 15.1 Hz]. ^{13}C NMR (150.90 MHz, CD_2Cl_2, 20 °C): 150.0 [d, C_α, ^2J(Tl–C) = 16 Hz]; 140.8 [d, C_1, ^4J(Tl–C) = 27 Hz]; 136.5 [d, ^5J(Tl–C) = 22 Hz] and 135.9 [d, ^5J(Tl–C) = 22 Hz] for phenyl-$C_{2,6}$; 122.9 (s, C_4); 132.7 [d, C_β, ^3J(Tl–C) = 116 Hz]; 130.2 (s, $C_{3,5}$); 121.2 [d, C_m, ^3J(Tl–C) = 146 Hz]. ^{13}C

NMR (150.90 MHz, CD_2Cl_2, −90 °C): δ 173.8 [d, OAc–CO, ^2J(Tl–C) = 242 Hz]; 148.4 [d, C_α, ^2J(Tl–C) = 16 Hz]; 139.3 [d, C_1, ^4J(Tl–C) = 27 Hz]; 135.7 [d, ^5J(Tl–C) = 22 Hz] and 135.5 [d, ^5J(Tl–C) = 27 Hz] for phenyl-$C_{2,6}$; 121.7 (s, C_4); 132.1 [d, C_β, ^3J(Tl–C) = 117 Hz]; 129.2 (s) and 129.1(s) for $C_{3,5}$; 120.2 [d, C_m, ^3J(Tl–C) = 146 Hz]; 17.6 [d, OAc–Me, ^3J(Tl–C) = 292 Hz].

2.5. Spectroscopy

^{1}H and ^{13}C NMR spectra in $CDCl_3$ or CD_2Cl_2 (99.6% from Aldrich) were recorded at 599.95, 600.1 or 499.85 and 150.87, 150.91 or 125.70 MHz, respectively, on Varian Unity Inova-600 Bruker DMX-600 or Varian Unity Inova-500 spectrometers locked on deuteriated solvent, and referenced to the solvent peak. ^{1}H NMR is relative to $CDCl_3$ or CD_2Cl_2, at $\delta = 7.24$ or 5.30 and ^{13}C NMR to the centre line of $CDCl_3$ or CD_2Cl_2 at $\delta = 77.0$ or 53.6. Next, the temperature of the spectrometer probe was calibrated by the shift difference of the methanol resonance in the ^{1}H NMR spectrum. Heteronuclear multiple quantum coherence was used to correlate protons and carbon through one-bond coupling and heteronuclear multiple bond coherence for two- and three-bond proton–carbon coupling.

IR spectra of **2** and $H_2(p\text{-Cl})_4$tpp were recorded at 25 °C in KBr discs on a Bruker EQUINOX 55 spectrometer.

The positive-ion fast atom bombardment mass spectrum (FAB MS) was obtained in a nitrobenzyl alcohol matrix using a JEOL JMS-SX/SX 102A mass spectrometer. UV–Vis spectra were recorded at 25 °C on a HITACHI U-3210 spectrophotometer.

2.6. Crystallography

Table 1 presents the crystal data as well as other information for **1**·$CHCl_3$, **2**·$CHCl_3$ and **3**·$CHCl_3$. Measurements were taken on a Bruker SMART CCD diffractometer using monochromatized Mo Kα radiation ($\lambda = 0.71073$ Å). The SADABS and the empirical absorption corrections were made for **1**·$CHCl_3$ and **2**·$CHCl_3$ (or **3**·$CHCl_3$), respectively. The structures were solved by direct methods (SHELXTL PLUS) and refined by the full-matrix least-squares method. All non-hydrogen atoms were refined with anisotropic thermal parameters, whereas all hydrogen atom positions were calculated using a riding model and were included in the structure factor calculation. Tables 2 and 3 list selected bond distances and angles for these three complexes.

3. Results and discussion

3.1. Molecular structures of 1·$CHCl_3$, 2·$CHCl_3$ and 3·$CHCl_3$

The molecular frameworks for complexes **1**–**3** are depicted in Figs. 1 and 2. Their structures are a six-coordinate thallium and a five-coordinate indium, having four nitrogen atoms of the porphyrins in common, but they are different with a chelating bidentate OAc^- ligand for **1**·$CHCl_3$ and a unidentate OAc^- ligand for **2**·$CHCl_3$ and **3**·$CHCl_3$. The metal–ligand bond distances, i.e. from the thallium(III) and indium(III) to the ligand and the angles are summarized in Tables 2 and 3.

Table 1
Crystal Data for **1**·$CHCl_3$, **2**·$CHCl_3$ and **3**·$CHCl_3$

Empirical formula [a]	$C_{47}H_{28}Cl_7N_4O_2Tl$ (**1**·$CHCl_3$)	$C_{47}H_{28}Cl_7InN_4O_2$ (**2**·$CHCl_3$)	$C_{47}H_{28}Br_4Cl_3InN_4O_2$ (**3**·$CHCl_3$)
Formula weight	1133.25	1043.70	1221.54
Space group	$P\bar{1}$	$P\bar{1}$	$P\bar{1}$
Z	2	2	2
Unit cell dimensions			
a (Å)	10.6430(8)	10.5984(6)	10.6153(6)
b (Å)	14.590(1)	14.6383(8)	14.7442(7)
c (Å)	15.550(1)	15.6115(9)	15.7201(8)
α (°)	67.776(1)	67.611(1)	68.296(1)
β (°)	77.501(1)	77.423(1)	77.541(1)
γ (°)	84.254(1)	84.266(1)	85.221(1)
V (Å^3)	2181.7(3)	2185.3(2)	2232.1(1)
D_{calc} (g cm^{-3})	1.725	1.586	1.817
Radiation, λ (Å)	Mo, 0.71073	Mo, 0.71073	Mo, 0.71073
Temperature (K)	293(2)	294(2)	295(2)
Absorption coefficient (mm^{-1})	4.175	1.014	4.334
R [b] (%)	3.36	3.57	4.28
R_w [c] (%)	9.93	9.36	10.15
Goodness-of-fit	0.866	1.026	0.943

[a] Including solvate molecules.
[b] $R = [\Sigma||F_o| - |F_c||/\Sigma|F_o|]$.
[c] $R_w = \{\Sigma[w(F_o^2 - F_c^2)^2]/\Sigma[w(F_o^2)^2]\}^{1/2}$; $w = A/(\sigma^2 F_o + BF_o^2)$.

Table 2
Selected bond lengths (Å) and angles (°) for **1**·$CHCl_3$ and **2**·$CHCl_3$

Compound **1**·$CHCl_3$			
Bond lengths			
Tl–O(1)	2.193(4)	Tl–N(1)	2.195(3)
Tl–O(2)	2.779(5)	Tl–N(2)	2.204(3)
C(45)–O(1)	1.172(8)	Tl–N(3)	2.186(3)
C(45)–O(2)	1.266(8)	Tl–N(4)	2.219(3)
C(45)–C(46)	1.541(9)		
Bond angles			
O(1)–Tl–O(2)	49.8(2)	N(1)–Tl–N(2)	84.2(1)
O(1)–C(45)–O(2)	124.7(6)	N(1)–Tl–N(3)	143.5(1)
O(1)–Tl–N(1)	100.9(2)	N(1)–Tl–N(4)	84.1(1)
O(1)–Tl–N(2)	122.7(2)	N(2)–Tl–N(3)	85.0(1)
O(1)–Tl–N(3)	114.2(2)	N(2)–Tl–N(4)	143.0(1)
O(1)–Tl–N(4)	93.9(2)	N(3)–Tl–N(4)	84.0(1)
O(2)–Tl–N(1)	126.6(2)	C(45)–O(2)–Tl	77.2(4)
O(2)–Tl–N(2)	81.4(1)	C(45)–O(1)–Tl	107.9(4)
O(2)–Tl–N(3)	85.8(2)		
O(2)–Tl–N(4)	132.6(2)		
Compound **2**·$CHCl_3$			
Bond lengths			
In(1)–O(1)	2.088(2)	In(1)–N(1)	2.148(2)
In(1)···O(2)	2.936(2)	In(1)–N(2)	2.139(2)
O(1)–C(45)	1.258(4)	In(1)–N(3)	2.170(2)
O(2)–C(45)	1.242(4)	In(1)–N(4)	2.150(2)
C(45)–C(46)	1.501(5)		
Bond angles			
C(45)–O(1)–In(1)	114.9(2)	N(1)–In(1)–N(2)	86.85(7)
O(1)–C(45)–O(2)	122.7(3)	N(1)–In(1)–N(3)	149.62(8)
O(1)–In(1)–N(1)	115.8(1)	N(1)–In(1)–N(4)	85.87(7)
O(1)–In(1)–N(2)	111.28(9)	N(2)–In(1)–N(3)	85.84(8)
O(1)–In(1)–N(3)	94.29(9)	N(2)–In(1)–N(4)	149.13(9)
O(1)–In(1)–N(4)	98.87(9)	N(3)–In(1)–N(4)	85.46(7)

Table 3
Selected bond lengths (Å) and angles (°) for **3**·$CHCl_3$

Compound **3**·$CHCl_3$			
Bond lengths			
In(1)–O(1)	2.083(3)	In(1)–N(2)	2.135(3)
In(1)···O(2)	2.907(3)	In(1)–N(3)	2.171(3)
In(1)–N(1)	2.151(3)	In(1)–N(4)	2.147(3)
Bond angles			
O(1)–In(1)–N(1)	115.9(1)	N(1)–In(1)–N(2)	87.0(1)
O(1)–In(1)–N(2)	111.1(1)	N(1)–In(1)–N(3)	149.4(1)
O(1)–In(1)–N(3)	94.4(1)	N(1)–In(1)–N(4)	85.5(1)
O(1)–In(1)–N(4)	99.4(1)	N(2)–In(1)–N(3)	85.7(1)
N(2)–In(1)–N(4)	148.9(1)	N(3)–In(1)–N(4)	85.7(1)

Bond distances (Å) are Tl–O(1) = 2.193(4), Tl–O(2) = 2.779(5), and the mean Tl–N(p) = 2.201(3) for **1**·$CHCl_3$; for **2**·$CHCl_3$ the values are In(1)–O(1) = 2.088(2), and the mean In(1)–N(p) = 2.152(2). Similarly, bond distances (Å) are In(1)–O(1) = 2.083(2) and the mean In(1)–N(p) = 2.151(3) for **3**·$CHCl_3$. Although the O(2) atom is at a 2.779(5) Å distance from the thallium, which is considerably longer than the Tl–O(1) distance, the interaction of the acetate with thallium in **1**·$CHCl_3$ is also classified as chelating bidentate. This classification is supported by a larger spread of Tl–O distances found in the crystal structure of thallium(III) acetate monohydrate, varying from 2.17(1) to 2.78(2) Å [5,6]. It is further substantiated by dimethyl(2-thioorotato)thallium(III) monohydrate, $TlMe_2Tot·H_2O$, which exhibited Tl–O distances ranging from 2.668(9) to 2.86(1) Å [7]. This type of bidentate interaction was also previously observed for Tl(N–Me–tpp)$(OAc)_2$ with Tl(1)–O(3) = 2.223(5) Å and Tl(1)–O(4) = 2.746(7) Å [8]. Hence all the oxygen atoms [i.e. O(1) and O(2)] are certainly coordinated to the thallium atom in **1**·$CHCl_3$.

The geometry around Tl in **1** is a distorted square-based pyramid in which the apical site is occupied by a chelating bidentate OAc^- group, whereas that around the In^{3+} in **2** and **3** is described as a regular squared-based pyramid with N(1), N(2), N(3) and N(4) lying in the basal plane. Because of the larger size of Tl^{3+}, Tl lies 0.69 Å above the 4N plane toward the acetate oxygen for **1**·$CHCl_3$, compared to 0.57 Å for In(1) in **2**·$CHCl_3$ and **3**·$CHCl_3$. The OAc^- ligand is bidentately coordinated to the Tl atom in **1**, **4** and Tl(tpp)(OAc) (Table 4). Moreover, the structure of **2** and **3** is quite different from that of In(tpp)(OAc) (Table 4). In In(tpp)(OAc), the OAc^- ligand is bidentately coordinated to the In atom whereas in **2** and **3**, it is unidentate. Such a difference in structure can be explained, that the tetra(*p*-chloro)- and tetra(*p*-bromo)-substitution favors the unidentate coordination either in **2** or in **3**. Similar observation is made for the trifluoroacetate ligand being unidentately coordinated to the Tl atom in Tl[(*p*-$Cl)_4$tpp](O_2CCF_3) whereas in Tl(tpp)(O_2CCF_3) it is chelating bidentate [9].

The dihedral angles between the mean plane of 4N and the planes of the phenyl groups are 43.9° [C(24)], 75.1° [C(30)], 69.5° [C(36)] and 49.4° [C(42)] for **1**·$CHCl_3$ and the corresponding angles are 69.7° [C(24)], 73.6° [C(30)], 47.5° [C(36)] and 49.6° [C(42)] for **2**·$CHCl_3$, and 70.1°, 73.2°, 48.7°, 47.9° for **3**·$CHCl_3$. The radii of the central 'hole' [Ct···N, the distance from the geometrical centre (Ct) of the mean plane of the 4N-atom core to the porphyrinato-core N atoms] are 2.09 Å for **1**·$CHCl_3$, 2.08 Å for **2**·$CHCl_3$ and 2.07 Å for **3**·$CHCl_3$ which are larger than 2.01 Å as suggested by Collins and Hoard [10]. The thallium(III) and indium(III) are bonded in a modestly expanded porphyrinato core ($C_{20}N_4$) in **1**·$CHCl_3$ and **2**·$CHCl_3$ (or **3**·$CHCl_3$), individually.

3.2. ^1H and ^{13}C NMR of complexes 1–4 in $CDCl_3$ and CD_2Cl_2

When a 0.02 M solution of **1** in CD_2Cl_2 (Fig. 3) was cooled, the methyl proton signals of OAc^-, being a single peak at 20 °C ($\delta = -0.02$ ppm), first broadened (coalescence temperature $T_c = -73$ °C) and then split

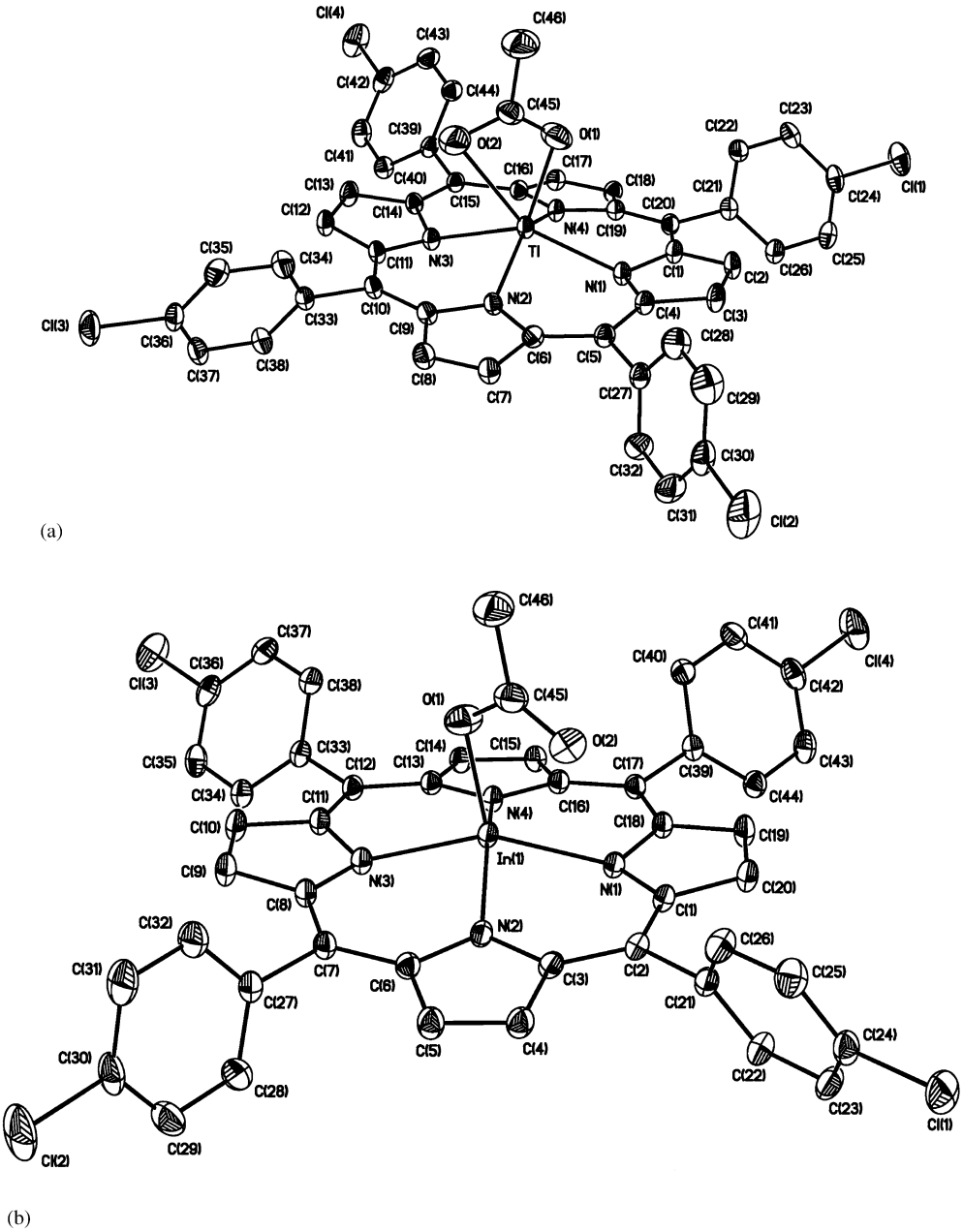

Fig. 1. Molecular configuration and atom-labelling scheme for (a) **1**·$CHCl_3$ and (b) **2**·$CHCl_3$, with ellipsoids drawn at 30% probability. Hydrogen atom and solvent $CHCl_3$ for both compounds are omitted for clarity.

into two peaks with a separation of 14.4 Hz at −90 °C. As the exchange of OAc^- within **1** is reversible, the results at 599.95 MHz confirm the separation as a coupling of ^4J(Tl–H). As a result of this observation, the most likely cause of loss of coupling should be due to reversible dissociation of acetate

$$Tl[(p\text{-}Cl)_4tpp](OAc) \rightleftharpoons Tl[(p\text{-}Cl)_4tpp]^+ + OAc^- \quad (1)$$

with a small dissociation constant and reasonable rate at room temperature. Such a scenario would lead to little change in the chemical shift with temperature and no detectable free OAc^- and $Tl[(p\text{-}Cl)_4tpp]^+$ at low temperature, but would lead to the loss of coupling between acetate and thallium at higher temperatures. The chemical shift in the high-temperature limit is the average for two species (i.e. $Tl[(p\text{-}Cl)_4tpp](OAc)$ and OAc^-) in Eq. (1) weighted by their concentration [11]. At −90 °C, the rate of intermolecular exchange of OAc^- for **1** in CD_2Cl_2 is slow and hence at low temperature, the CO and CH_3 of OAc^- in **1** are observed at 173.8 ppm [with ^2J(Tl–C) = 242 Hz] and 17.7 ppm [with ^3J(Tl–C) = 292 Hz], respectively. At 20 °C, intermolecular exchange of the OAc^- group is rapid, indicated by singlet signals due to carbonyl

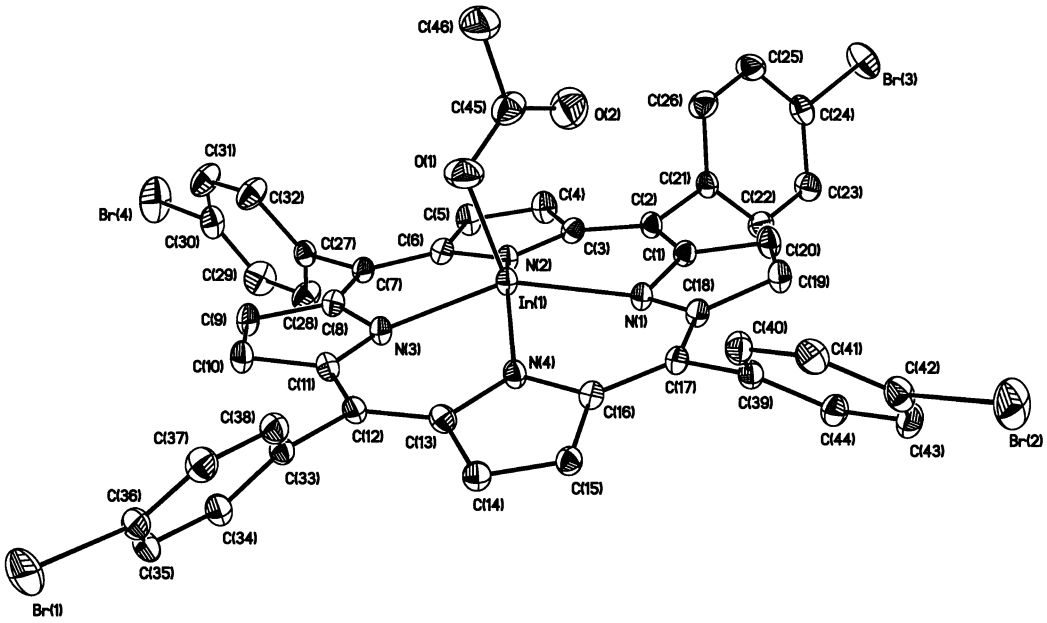

Fig. 2. Molecular configuration and atom-labelling scheme for **3**·$CHCl_3$, with ellipsoids drawn at 30% probability. Hydrogen atom and solvent $CHCl_3$ are omitted for clarity.

carbons at 173.7 ppm and methyl carbons at 18.3 ppm. The free energy of activation $\Delta G^{\neq}_{200} = 42.54$ kJ mol^{-1} is therefore determined for the intermolecular exchange of OAc^- in **1**. Similarly, $\Delta G^{\neq}_{200} = 42.46$ kJ mol^{-1} is evaluated for the intermolecular exchange of OAc^- in **4**.

The interaction of the carboxylate with the indium of **2** in the solid is purely unidentate, the second carboxylate oxygen, i.e. O(2), being 2.936(2) Å from the indium atom. This finding further confirms the IR spectroscopic method's effectiveness in assigning a bonding type in metalloporphyrin carboxylates [12]. Comparing the vibrational frequencies of **2** with those of $H_2(p\text{-Cl})_4$tpp allows for the bonds to be assigned at 1619 [$\nu_{asym}(CO_2)$] and 1207 [$\nu_{sym}(CO_2)$]. Herein, the frequency difference ($\Delta\nu$) between the asymmetric (ν_{asym}) and symmetric (ν_{sym}) C–O vibrations is 412 cm^{-1}. This $\Delta\nu$ value that is significantly greater than those of the ionic complex denote a unidentate formation [12]. In addition, X-ray diffraction analysis unambiguously confirms that **2** is a unidentate complex. In a series of tetraarylporphyrins with Ga, In, Tl, Ge or Sn as the central metal atom, ^{13}C NMR chemical shifts were shown to be a useful tool for diagnosing whether acetato ligands were unidentate or bidentate. Unidentate acetato ligands were located at 20.5 ± 0.2 and 168.2 ± 1.7 ppm and the bidentate acetato ligands at 18.0 ± 0.7 and 175.2 ± 1.6 ppm [3]. The methyl and carbonyl chemical shifts of the acetato group for **2** in $CDCl_3$ at 20 °C are separately located at 18.2 and 176.0 ppm (Table 4) suggesting that the acetate is asymmetrically chelating bidentate coordinated to the indium atom in **2** in the solution phase (Eq. (2))

Table 4
^{13}C NMR and X-ray data of the acetato group on the M[(p-X)$_4$tpp](OAc) complexes with M = In, Tl and X = Cl, Br

Compound	X-ray (Å) $\Delta l = l_2 - l_1$			Solid carboxylate binding, found	Solution ^{13}C NMR (ppm)		Solution carboxylate binding [b]
	M–O	M–O′(M···O′)	Δl [a]		δ(CO)	δ(CH_3)	
Tl(tpp)(OAc)	2.299	2.361	0.062	bidentate	173.1	18.5	bidentate
Tl[(p-Cl)$_4$tpp](OAc) (**1**)	2.193	2.779	0.586	bidentate	173.8	17.7	bidentate
Tl[(p-Br)$_4$tpp](OAc)[13] (**4**)	2.352	2.380	0.028	bidentate	173.8	17.6	bidentate
	2.38	2.41	0.03				
In(tpp)(OAc)	2.215	2.322	0.107	bidentate	176.1	18.1	bidentate
In[(p-Cl)$_4$tpp](OAc) (**2**)	2.088	2.936	0.848	unidentate	176.0	18.2	bidentate
In[(p-Br)$_4$tpp](OAc) (**3**)	2.083	2.907	0.824	unidentate	176.3	18.1	bidentate

NMR data were recorded in CD_2Cl_2 at −90 °C for **1**, **4** and in $CDCl_3$ for **2**, **3** at 20 °C.
[a] Let M–O = l_1, M–O′ (or M···O′) = l_2 and $\Delta l = l_2 - l_1 > 0$.
[b] The structure was obtained by prediction based on Ref. [3].

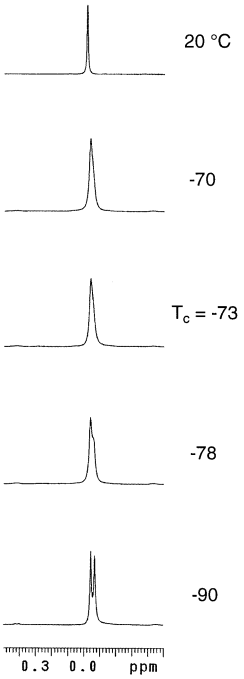

Fig. 3. The 599.95 MHz ^{1}H NMR spectra for the axial acetato protons of Tl[(p-Cl)$_4$tpp](OAc) (**1**) in CD_2Cl_2 at various temperatures.

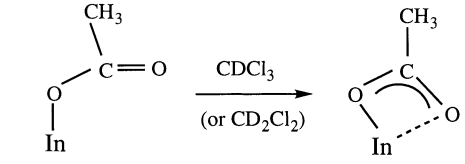

solid (unidentate) solution asymmetrically chelating bidentate

(2)

A similar phenomenon was found for In(p-Br)$_4$tpp(OAc) (**3**). The OAc^- ligand is unidentately coordinated to the In atom for **3** in the solid phase and asymmetrically chelating bidentate bound to the indium in the solution phase (Table 4). Moreover, the OAc^- ligand is bidentately coordinated to the indium atom for In(tpp)(OAc) both in the solid and the solution phase (Table 4).

In conclusion, this work describes one new thallium complex **1** and two new indium complexes **2** and **3**, characterized by spectroscopic and crystallographic methods. Dynamic ^{13}C and ^{1}H NMR spectra for the acetato group of **1** and **4** in CD_2Cl_2 reveal that the OAc^- group undergoes intermolecular exchange with a free energy of activation $\Delta G^{\neq}_{200} = 42.54$ kJ mol^{-1} for **1** and $\Delta G^{\neq}_{200} = 42.46$ kJ mol^{-1} for **4**.

4. Supplementary material

Crystallographic data in CIF format for **1**, **2** and **3** have been deposited with Cambridge Data Centre as CCDC 200322, 200323 and 200324, respectively. Copies of this information may be obtained free of charge from The Director, CCDC, 12 Union Road, Cambridge, CB2 1EZ, UK (fax: +44-1223-336033; e-mail: deposit@ccdc.cam.ac.uk or www: http://www.ccdc.cam.ac.uk).

Acknowledgements

Financial support from the National Research Council of the ROC under Grant NSC 91-2113-M-005-015 is gratefully acknowledged.

References

[1] J.C. Chen, H.S. Jang, J.H. Chen, L.P. Hwang, Polyhedron 10 (1991) 2069.
[2] S.C. Suen, W.B. Lee, F.E. Hong, T.T. Jong, J.H. Chen, L.P. Hwang, Polyhedron 11 (1992) 3025.
[3] S.J. Lin, T.N. Hong, J.Y. Tung, J.H. Chen, Inorg. Chem. 36 (1997) 3886.
[4] M. Inamo, N. Kamiya, Y. Inoda, S. Funahashi, M. Nomura, Inorg. Chem. 40 (2001) 5636.
[5] R. Faggiani, I.D. Brown, Acta Crystallogr., Sect. B 38 (1982) 2473.
[6] M.O. Senge, K.R. Senge, K.J. Regli, K.M. Smith, J. Chem. Soc., Dalton Trans. (1993) 3519.
[7] M.S. Garcia-Tasende, B.E. Rivero, A. Castineiras, A. Sanchez, J.S. Casas, J. Sordo, W. Hihler, J. Strahle, Inorg. Chim. Acta 181 (1991) 43.
[8] J.Y. Tung, J.H. Chen, F.L. Liao, S.L. Wang, L.P. Hwang, Inorg. Chem. 39 (2000) 2120.
[9] Y.Y. Lee, J.H. Chen, H.Y. Hsieh, F.L. Liao, S.L. Wang, J.Y. Tung, S. Elango, Inorg. Chem. Commun. 6 (2003) 252.
[10] D.M. Collins, J.L. Hoard, J. Am. Chem. Soc. 92 (1970) 3761.
[11] J.P. Jensen, E.L. Muetterties, in: L.M. Jackman, F.A. Cotton (Eds.), Dynamic Nuclear Magnetic Resonance Spectroscopy, Academic Press, New York, 1975, pp. 299–304.
[12] G.B. Deacon, R.J. Phllips, J. Coord. Rev. 33 (1980) 227.